JOURNAL OF GEOPHYSICAL RESEARCH, VOL. 117, D09202, doi:10.1029/2011JD016696, 2012

An observational study of aerosol and turbulence properties during dust storms in northwest China

Peijian Fu,[1,2] Shiyuan Zhong,[3] Jianping Huang,[1,2] and Guangning Song[1,2]

Received 8 August 2011; revised 23 March 2012; accepted 23 March 2012; published 2 May 2012.

[1] Since late 2003, measurements of aerosol properties and meteorology have been made at three sites, Minqin, Jiuquan and Dunhuang, in the border areas of the Gobi and Taklimakan Deserts in the northwest of China as part of an observational program for Asian Dust Storms (ADS). The aerosol observations include mass concentration and optical depth, and the meteorological observations include both mean and turbulent quantities. The data from a three-year period (2004–2007) have been analyzed to characterize aerosol and meteorological conditions during dust storms. The results show that during ADS the aerosol mass concentration (PM_{10}) can reach above 7~8 mg m^{-3}, 10~100 times of that on clear days, and the scatter coefficient of fine particles ($PM_{2.5}$) is 2000~2500 10^{-6} m^{-1}, 20~25 times of the clear day values. There is a dramatic reduction in the visibility during dust storms with average visibility about 2 km, which is only 1/20~1/30 of that on clear days. The aerodynamic roughness is 0.018 and 0.046 m for the Taklimakan and Gobi Deserts respectively, and the friction velocity is about 0.71 and 0.56 m s^{-1} during ADS periods, doubling the value found on quiescent days. Turbulence in the lower atmosphere is more intense during ADS period due mainly to increased vertical wind shear associated with strong winds. The large-scale circulation patterns show that during the ADS conditions the Gobi Desert is typically in the path of cold air from high latitudes moving toward the south or southeast and the data suggest that there is a declining trend for dust storms during the past 5 decades.

Citation: Fu, P., S. Zhong, J. Huang, and G. Song (2012), An observational study of aerosol and turbulence properties during dust storms in northwest China, *J. Geophys. Res.*, *117*, D09202, doi:10.1029/2011JD016696.

1. Introduction

[2] Commonly in late winter and spring, as cold and dry continental polar air mass from northern latitudes moves southward or south-southeastward to exchange heat and moisture with warm and moist air mass at lower latitudes, the two different air masses meet in Mongolia or Inner-Mongolia of China to form the cold front or cold air outbreak [*Wang et al.*, 2008; *Sun et al.*, 2001]. Given suitable atmospheric conditions, the strong surface winds associated with the baroclinic system of cold front lift dust from the dry sandy surface of the deserts in western China to produce so-called Asian Dust Storms (ADS).

[3] *Sun et al.* [2001] statistically analyzed the moving route of cold front or cold air outbreak which generated the dust storms over Gobi Desert in the past 40 years. They showed a map of typical dust storm trajectories, which is consistent with the results of the other researchers [*Kim*, 2008; *Chen et al.*, 2008; *Kim et al.*, 2008]. *Aoki et al.* [2005] studied dust storms in Tarim Basin and found that they can be generated by strong mesoscale wind systems found in the synoptic-scale cold air mass behind cold fronts coming to the Tarim Basin from north. So the strong wind associated with cold front or cold air outbreak is the basic condition for ADS in western China.

[4] When cold fronts move down to the south, passing desert areas, they may cause the surface wind speed to increase to about 8–10 ms^{-1} and temperature to drop more than 10°C in local areas. The strong wind then lift dusts from the ground. Occasionally, cold fronts also bring a little rain or snow, but most of time they do not produce any precipitation because the air is typically cold and dry during the season of frequent ADS and raindrops generated from frontal clouds may evaporate completely before reaching the ground.

[5] Once elevated to the upper troposphere, dust aerosols may be caught by the westerly jet streams and be transported rapidly downstream from Asia across the Pacific Ocean, producing dust aerosol pollution over Western North

[1]Key Laboratory of Arid and Semi-Arid Climate, Lanzhou University and Ministry of Education, Lanzhou, China.
[2]College of Atmospheric Sciences, Lanzhou University, Lanzhou, China.
[3]Department of Geography and Center for Global Climate Change and Earth Observations, Michigan State University, East Lansing, Michigan, USA.

Corresponding Author: P. Fu, College of Atmospheric Sciences, Lanzhou University, Lanzhou 730000, China. (fupj@lzu.edu.cn)

0148-0227/12/2011JD016696

America [*Xuan et al.*, 2004; *Zhang*, 2001; *VanCuren and Cahill*, 2002; *Roberts et al.*, 2006; *Huang et al.*, 2007, 2009; *Wang et al.*, 2008]. Utilizing satellite and weather observational data, researchers have studied the mechanisms for ADS formation [*Qian et al.*, 2006; *Ye et al.*, 2000], their transport pathways [*Kim*, 2008; *Chen et al.*, 2008; *Kim*, 2008], and the environmental impacts of ADS on the downstream regions such as Korea, Japan, north Pacific and the United States [*In and Park*, 2002; *Park and In*, 2002; *Lee et al.*, 2008; *Wang et al.*, 2010; *Huang et al.*, 2009, 2010].

[6] The ADS not only have direct effects on the climate through reflection and absorption of short- and longwave radiation [*Ge et al.*, 2010; *Huang et al.*, 2008] but also modify cloud properties [*Huang et al.*, 2006a, 2006b, 2006c; *Su et al.*, 2008]. In addition, the ADS accelerates desertification, influences local climate, severely affects human life and causes casualties [*Jigjidsuren and Oyuntsetseg*, 1998; *Huang et al.*, 2010]. Because of its large impact on the atmospheric environment, ADS has attracted scientific attention in recent decades [*Natsagdorj et al.*, 2003; *Huebert et al.*, 2003]. A number of important questions have been raised about ADS: Is there regularity for ADS? What is the variation of ADS in the past decades? How will ADS change under various global climate change scenarios? To answer these questions researchers have performed a number of studies that analyzed meteorological data and modeled the atmospheric circulation fields over western China, but systematic observations of ADS especially in the source areas is necessary in order to comprehend the entire dust storm process. Since the sources of ADS are usually found in remote areas, such observations are difficult to make. Questions about the characteristics of ADS and the accompanying atmospheric conditions at local, regional and global scales still remain unanswered. Understanding these questions is of particular significance for validating satellite observations and for understanding climate and climate change in arid regions.

[7] To understand dust aerosol properties and the near-surface atmospheric conditions over the source region, observations have been made in the regions near the Gobi and Taklimakan Deserts. These observations include measurements of the dust aerosol mass concentration and its variation, and the mean and turbulent characteristics in the surface layer. Upper-air atmospheric data have also been archived to understand atmospheric circulation patterns during ADS.

2. Sources of Dust Storms, Observation Location, Measurements and Data Set

2.1. Two Major Sources of Dust Storms in China: Gobi and Taklimakan Deserts

[8] Cenozoic tectonic uplift controls global climate changes. The uplift of the Tibetan Plateau is the basic force of climate changes in western China. The Tibetan Plateau alters the westerly wind circulation, leading to enhanced rainfall on the west and southwest side of the plateau and remarkable reduction of rainfall in basins on the north and northeast side. The uplift of the Tibetan Plateau also enhances Siberian – Mongolian high pressure, causing extraordinary dryness in northwest China [*Li et al.*, 2006]. Thus the uplift of the Tibetan Plateau is the basic reason for the arid basins on its north and northeast side. Quaternary Aeolian sediments are the chief materials of sandy desertification in Gobi and Taklimakan.

[9] The Gobi Desert is composed of two parts, Tengger and Badain Jaran. Both are located between northwestern China and Mongolia and cover an area of 36,700 km^2 and 47,000 km^2, respectively, ranging in 37°–42°N and 98.5°–106°E, with an altitude of 1200–1700 m MSL. There are some oases between and near them. Badain Jaran is located to the north of Tengger and extends to the north. Somewhere the two merge near Minqin. Temperature in the region experiences a large seasonal and daily variation, with an annual average lower than 10°C. The region is characterized by arid climate with plenty of sunshine on clear days and an annual average relative humidity of about 40%. When a cold air outbreak happens, the cold, dry air masses from the north polar latitudes sweep southward or southeastward through the Gobi Desert to China or eastern Asia. It is a chief source region for ADS.

[10] The Taklimakan Desert is located in the center part of Tarim basin in Western China, ranging 37°–41°N and 78°–90°E and covering 330,000 km^2, with the Kunlun Mountains and Tibetan Plateau to its south and the Altai Mountains and Tianshan Range to its north. The climate of the Taklimakan Desert is similar to that of Gobi. The Altai Mountains and Tianshan Range help block the lower-level airflow from entering the region from the north, resulting in calmer near-surface conditions and fewer ADS in the Taklimakan Desert compared to the Gobi Desert.

2.2. Observation Location

[11] The observational sites are located in the border areas between the Gobi Desert and the Taklimakan Desert (Figure 1) [*Tsai and Chen*, 2006].

[12] The three sites are: Minqin (38.63N, 103.08E, 1367 m above mean sea level or MSL), Jiuquan (39.77N, 98.48E, 1477 m MSL) and Dunhuang (40.15N, 94.68E, 1139 m MSL). Minqin is on the southern margin of the Gobi Desert, Dunhuang is close to the eastern boundary of the Taklimakan Desert, and Jiuquan is between the two sites (Figure 1). The distances are 460 km between Minqin and Jiuquan, and 330 km between Jiuquan and Dunhuang. The observations at the three sites are part of a long-term ADS monitoring program that was initiated in late 2003.

2.3. Measurements and Data Set

[13] At each site, aerosol properties are monitored using a TEOM 1400a particulate mass concentration PM_{10} monitor from Rupprecht & Patashnick, a FD12 visibility meter from Vaisala, and an Ecotech M9003 integrating nephelometer. Two 20-m micrometeorological towers are deployed at Minqin and Dunhuang. Each tower is instrumented at 5 levels (1, 2, 4, 10 and 20 m) with sensors for wind speed (014A-L, Met One) and direction (034B-L, Met One), temperature and humidity (HMP45C-L, Vaisala). The sampling frequency for aerosol monitors is once every 5 min and for tower observations is once every 10 s.

[14] In addition to the special measurements described above, hourly routine meteorological data are used to derive climatology of dust storms. To link the near-surface measurements to large-scale conditions, the gridded 6-hourly NCEP (National Center for Environmental Prediction, USA)

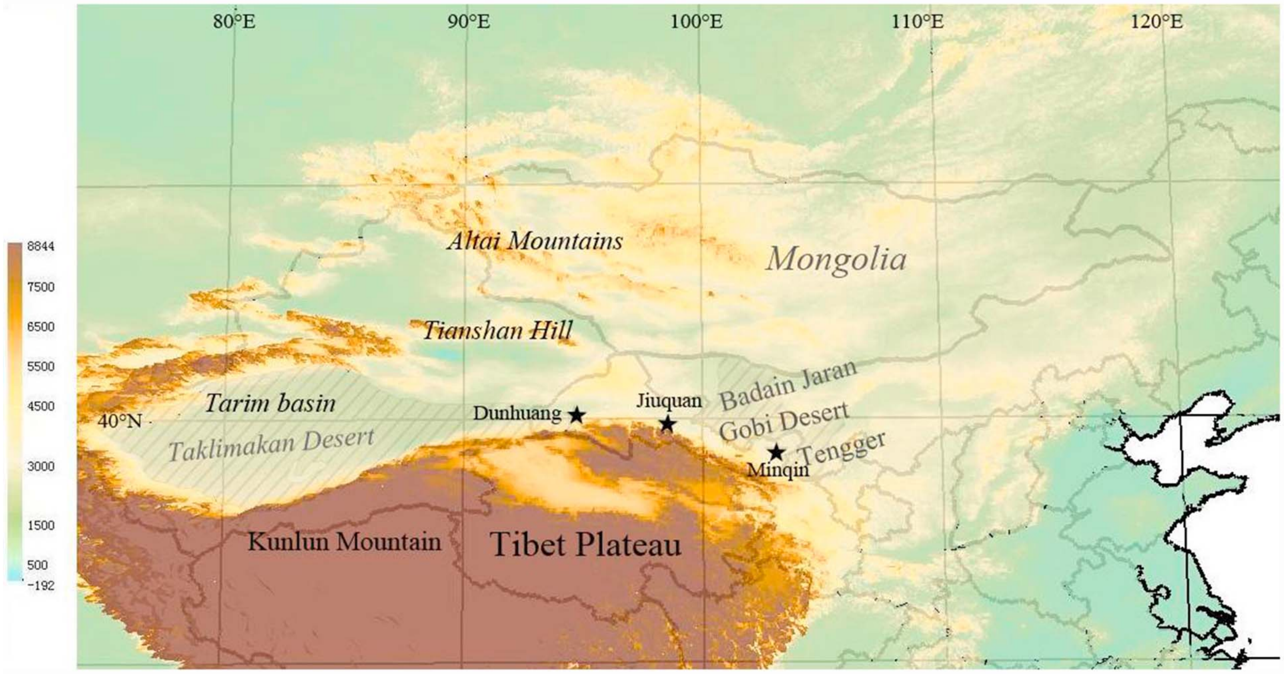

Figure 1. The Gobi Desert and Taklimakan Desert (with slant lines), regional topography, and the three observational sites (positioned with stars).

global reanalysis data [*Kalnay et al.*, 1996] are also used in this study for analyzing large-scale circulation patterns. The former include wind speed and direction, temperature, humidity, precipitation, visibility, and frequencies and durations of dust storms. The latter include meteorological elements at different levels in the troposphere. Both data sets extend back for more than 50 years.

[15] The time used in this study is Beijing time, which is 8 h ahead of Universal Coordinated Time (UTC). The local time at observational sites is almost 7 h ahead of UTC.

3. Data Analyses and Results

3.1. Dust Storm Climatology

[16] Climatology of dust storms is derived using 53 year (1954–2006) routine hourly meteorological observations of ADS. A dust storm was recorded when the visibility was less than 2 km under strong wind conditions. According to the formula of *Yang et al.* [2006] established for desert areas, visibility less than 2 km corresponds to heavy load of PM_{10} concentration above 5 mg m^{-3}. A dust storm day is defined as when there is at least one dust storm occurring on that day.

[17] During the 53-year (1954–2006) period, the total number of dust storm days was 534 at Jiuquan, 614 at Dunhuang, and 1515 at Minqin. Of these dust storm days, there were 254 concurrent days at Minqin and Jiuquan, approximately 17% of total dust storm days at Minqin. The concurrent days of Dunhuang and Jiuquan were 116, about 19% of total dust storm days at Dunhuang. The small percentage of the concurrent days among the three stations suggests that approximately 80% of dust storms only affected a small area of less than 300–400 km in radius. A dust storm may be of small or meso-scale characteristics in the lower troposphere, but as the dusts are carried into mid to upper troposphere, they can travel thousands of kilometers by prevailing wind aloft.

[18] Figure 2 shows the monthly averages of both the duration and frequency of dust storms at the Minqin, Dunhuang and Jiuquan sites. Also shown in Figure 2 are several meteorological elements known to affect dust storms (e.g., wind velocity, humidity and precipitation). At Minqin and Dunhuang, the duration and frequency of dust storms both peak in the spring, with maximum value in April for Minqin and Jiuquan, and in March for Dunhuang. The duration and frequency are low in autumn following the rainy season which runs from June to September and receives more than 70% of the annual total precipitation, with a minimum dust storm frequency occurring in September near the end of the rainy season. For most months of the year, the monthly duration and frequency of occurrence at Minqin more than double those at Dunhuang.

[19] The average duration of a dust storm can be obtained by dividing the monthly mean duration by monthly frequency. At Minqin the average duration for a dust storm from May through August is about 1–2 h and it is about 3 h during the rest of the year (not shown). At Dunhuang, the average duration is less than 2 h. The higher frequency and longer duration in the early spring (March–April) are accompanied by lower relative humidity and higher mean wind speed during this season, while the lower dust storm frequency and shorter duration in the fall season appear to correspond to lower wind speed and higher humidity in this season.

3.2. Dust Storm Characteristics

[20] Enhanced observational data during the three-year (2004–2006) period are analyzed to determine the characteristics of dust storms. The major characteristics are

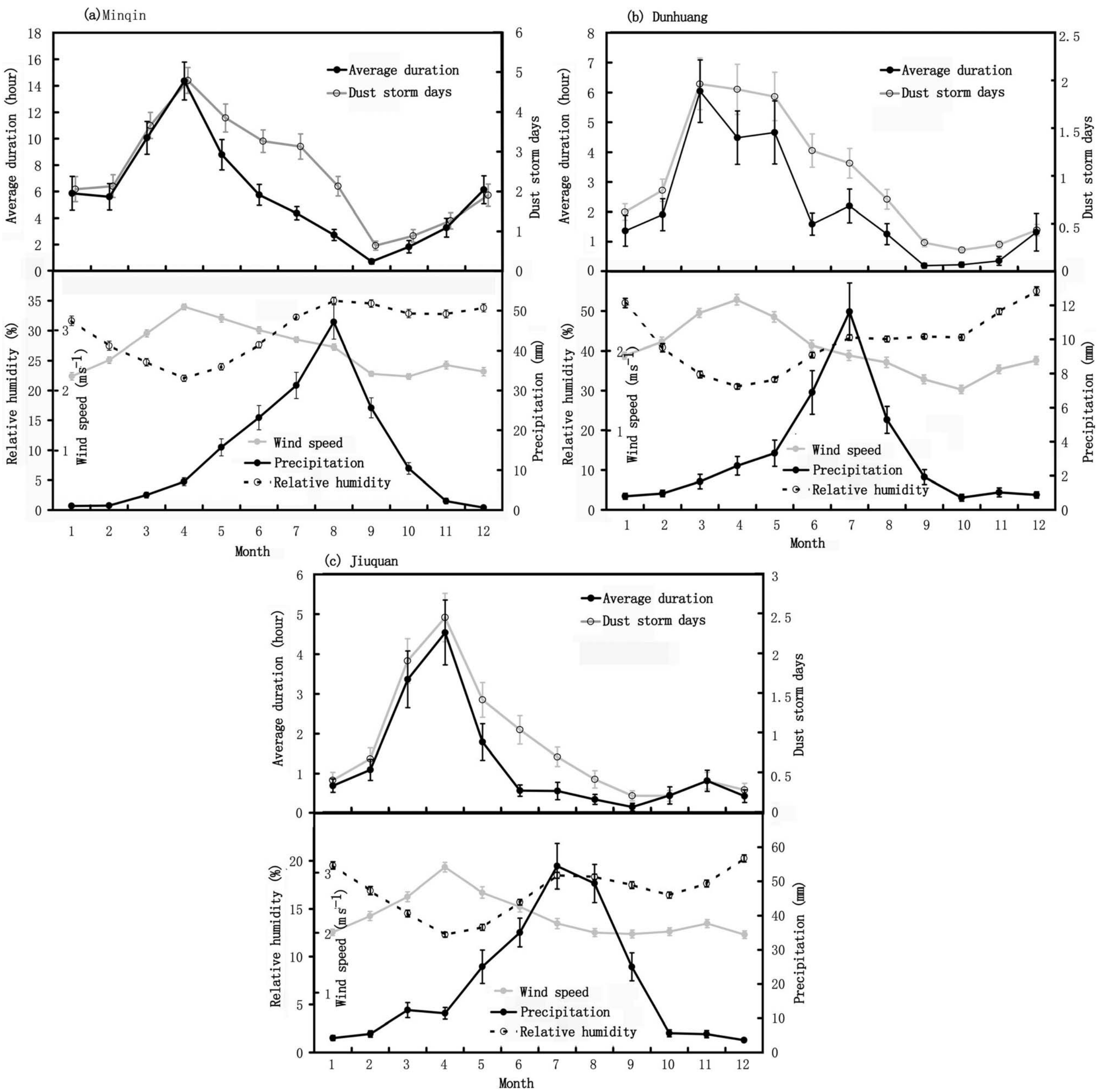

Figure 2. Monthly mean and standard error of the dust storm days and duration (h) and surface wind speed, relative humidity, and precipitation averaged over 1954–2006 for (a) Minqin, (b) Dunhuang and (c) Jiuquan.

summarized in Table 1. A dust storm is defined as a strong storm if it lasted longer than the three-year average. The three - year averages of dust storm duration are 1.23 and 1.18 h at Jiuquan and Dunhuang, while the average duration at Minqin is longer at 2.01 h. From Jan. 2004 to Dec. 2006, 39 dust storms occurred at Minqin, including 14 strong ones, 13 at Dunhuang including 5 strong ones, and 7 at Jiuquan with 3 strong ones. In this period the average duration of dust storms at Minqin is also 2 times of that at Dunhuang, consistent with the climatology based on 53-year routine observations. The dust storm frequency at Minqin is 3 times of that at Dunhuang. This result indicates that dust storms are more frequent in the Gobi Desert than in the Taklimakan Desert.

[21] Despite the differences in the frequency and duration of the dust storms among the three sites and between the two deserts, the aerosol characteristics, as measured by the concentration of dust aerosol, visibility and scatter coefficient, exhibit little difference among the three sites. The results show that some strong dust storms can reach the peak mass concentration (PM_{10}) above 7∼8 mg m^{-3}, which is 10∼100 times of that on clear days. There is a dramatic reduction in the visibility during dust storms with average visibility only about 2 km, 1/20∼1/30 of that on clear days. Scatter coefficient of fine particles ($PM_{2.5}$) are 2000∼2500 10^{-6} m^{-1},

Table 1. Observed Dust Storm Properties at the Three Sites (Jan. 2004–Dec. 2006)[a]

	Minqin	Jiuquan	Dunhuang
Duration of a dust storm (hours)	2.01 ± 1.46	1.23 ± 0.44	1.18 ± 0.83
Total dust storm events (strong[b])	39 (14)	7(3)	13 (5)
Mass concentration (mg m^{-3})	2.50 ± 2.12	2.33 ± 3.23	2.45 ± 2.67
Visibility (km)	2.08 ± 1.03	2.05 ± 2.31	2.11 ± 1.56
Scatter coefficient (M m^{-1})	2385.76 ± 2327.55	2053.12 ± 1530.01	22395 ± 891.20
Wind speed (m s^{-1})	11.27 ± 1.85	9.12 ± 2.33	10.32 ± 3.45
Relative humidity (%)	45.80 ± 6.45	48.65 ± 7.66	35.86 ± 3.23

[a]Measured quantities are averaged in the period of dust storms.
[b]A strong event of sand storm means its duration above the average one.

20∼25 times of the clear day values. PM_{10} concentration, scattering coefficient and visibility are relatively well correlated when concentration is higher than 5 mg m^{-3} and visibility is less than 2 km, especially the former two (Figure 3). But when concentration is less than 2 mg m^{-3}, the correlations between them are poor (r ≈ 0.3).

[22] Figure 4 shows a time series of PM_{10} concentration measured at the three locations from March 1 to May 31 in 2006. The dust storms were recorded asynchronously among three locations in most of the time. During the three-month period there were 5 large peaks with PM_{10} greater than 5 mg m^{-3} (heavy load of dust aerosol) at Minqin, 4 at Dunhuang and 1 at Jiuquan. On Mar 9, 2006, a spike of PM_{10} up to 5 mg m^{-3} was recorded at Minqin, a small peak of less than 2 mg m^{-3} at Jiuquan, but almost no peak at all at Dunhuang. Corresponding to the differences of PM_{10} among the three sites were the circulations of lower atmosphere (Figure 5). Strong northerly winds cross isotherms toward south bringing colder air over Gobi, while Dunhuang was relatively quiescent. However, there were also synchronous dust storms at the three locations, such as on April 10, 2006. On this day, wind vectors cross isotherms on a larger scale, covering both Taklimakan and Gobi (Figure 6) and the strong winds resulted in large peaks of PM_{10} at all three observational sites. The close relationship between 10-m level wind speed and PM_{10} can be clearly seen by the time series of the two parameters in Figure 7 for the peak dust storm month (April for Minqin and March for Dunhuang as shown in Figure 2). For 2005, data from May instead of April was shown for Minqin because there were some missing data at this site for April (Figure 7a).

[23] When PM_{10} was greater than 5 mg m^{-3}, daily mean wind speed was usually more than 8 m s^{-1} at 10-m level, such as on April 25 and 28, 2004, May 28, 2005, and April 10 and 24, 2006 at Minqin. But the reverse of the rule was not always true. Daily wind speed was above 8 m s^{-1} on April 30, 2004, May 14, 2005, and April 5–6, 2006, while the PM_{10} was about or less than 5 mg m^{-3} and even less than 3 mg m^{-3} on April 16–18 and 27–29, 2006 in the same dry season. Some other factors, such as soil wetness and gustiness, may also play a role in the development of dust storm events.

[24] The relationship between the PM_{10} concentration and wind speed at Dunhuang is shown in Figure 7b. There was a heavy load of PM_{10} (with peak above 5 mg m^{-3}) in both March of 2005 and 2006, but no large peak in March 2007 when the wind speed was less than 8 m s^{-1} for the whole month. A strong wind over the surface is a necessary condition for a dust storm with heavy load of PM_{10}. Under neutral conditions, friction velocity, which is a measure of surface stress, is determined by wind speed and surface roughness (refer to equation (1) below). When the roughness

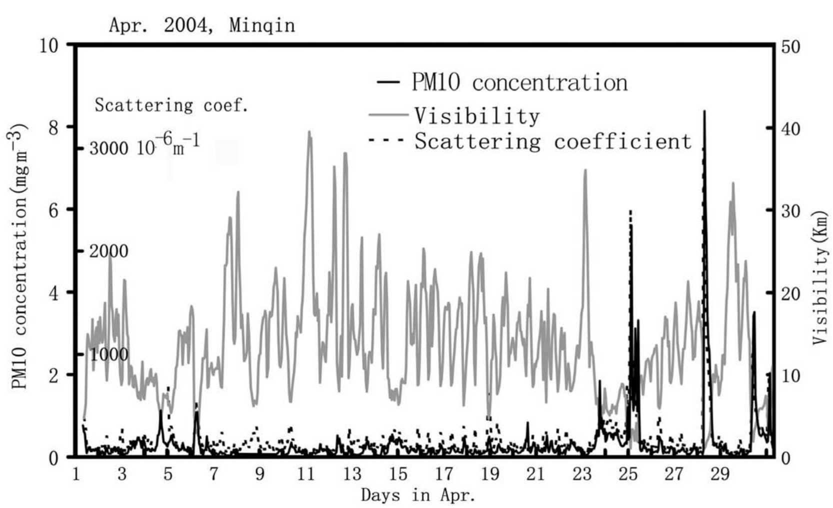

Figure 3. Time series of PM_{10} concentration, scattering coefficient and visibility (hourly averaged).

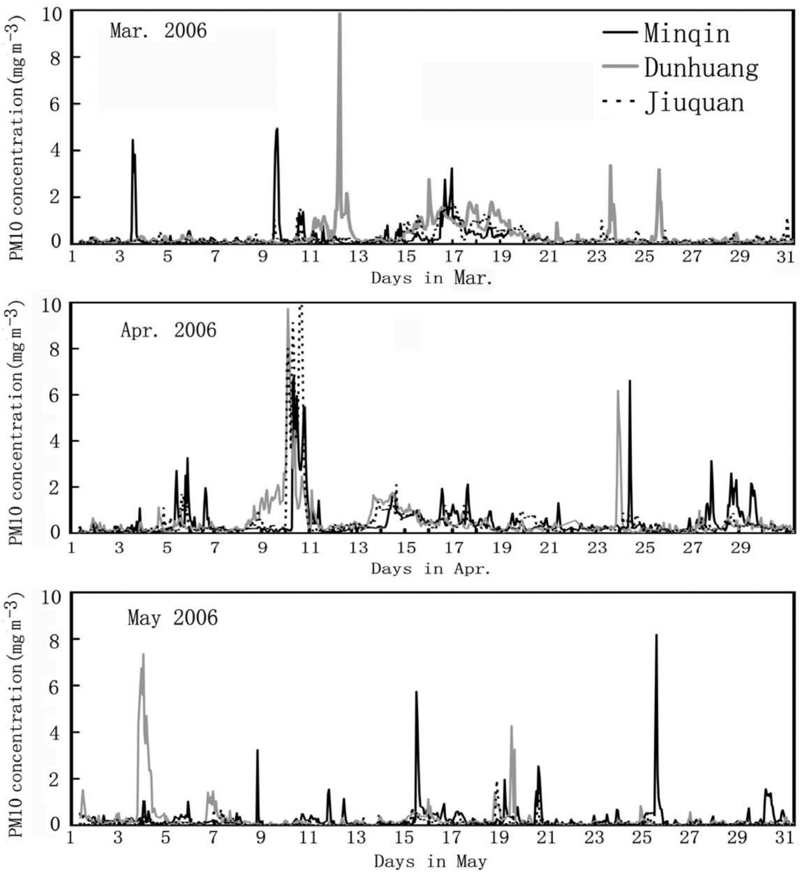

Figure 4. Time series of PM_{10} concentration for Mar 1–May 31 in 2006 (hourly averaged).

on the desert area is about 0.018–0.046 cm (see the following section), the wind speed of 8 m s^{-1} or above corresponds to a friction velocity of 0.56–0.71 m s^{-1} in neutral condition, which is consistent with the threshold friction velocity of 0.60 m s^{-1} set by *Westphal et al.* [1988] for dust storms in Saharan desert. Based on measurements of four dust storm events in April, 2006, *Li and Zhang* [2011] arrived at an estimate of 0.34–0.42 m s^{-1} as threshold friction velocity for dust storms over Gobi Desert which, as they noted, was lower than the results from other researchers. The difference between ours and their threshold values could be caused by the difference in the strengths of the dust storm events. The four events in their study are relatively weak with smaller dust mass concentration and area coverage compared to the events in our study.

[25] Figure 8 shows the peak concentration of PM_{10} with heavy load as a function of wind speed. Also shown in Figure 8 are the PM_{10} concentrations 1 and 2 h before and after the peak concentration was reached. For all 21 dust storms examined, the peak PM_{10} concentrations vary between 5 and 11 mg m^{-3} and all occurred when wind speeds are above 8 m s^{-1}. The concentrations increase rather quickly within the 2 h prior to the peak value. In comparison, the drop from the peak happens at a slower pace. This asymmetry may be caused by more dust particles from distant sources being advected into the area or the tendency for particles to be suspended in the air once brought up from the ground.

3.3. Wind Fields and Turbulent Characteristics During Dust Storms

[26] The flow dynamical and turbulence characteristics in the surface layer are very important for dust storms over the two deserts. During dust storms the average wind speed at the 10-m level above the ground was 8–11 m s^{-1} (Table 1), which yields a vertical wind shear of near unity, or $\partial\bar{u}/\partial z \sim 1/s$, and a gradient *Richardson* number $Ri = \frac{g}{\theta}\frac{\partial\bar{\theta}/\partial z}{\left(\partial\bar{u}/\partial z\right)^2} \sim 0.035\,\partial\bar{\theta}/\partial z$, the vertical temperature gradient usually satisfies the condition that $\left|\partial\bar{\theta}/\partial z\right| \ll 1\,\mathrm{K\,m^{-1}}$, resulting in $Ri \to 0$. This suggests that the mechanical turbulence production is more important than buoyancy production during dust storms and the atmosphere stability is near neutral. This can be clearly seen in Figure 9 that shows a close agreement between the observed wind speed profile during dust storms and a theoretical profile under neutral atmospheric stability condition.

[27] Based on the Monin-Obukhov similarity theory, the statistical quantities of turbulence may be estimated using mean profile data. *Businger et al.* [1971] and *Dyer* [1974]

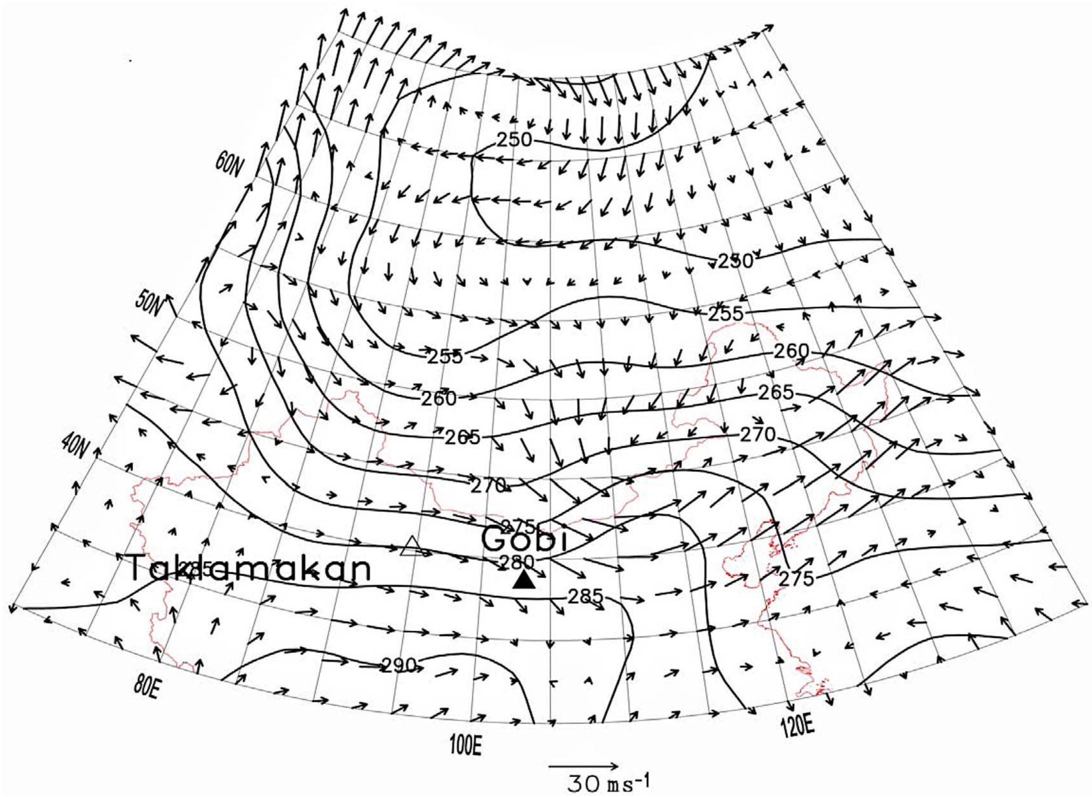

Figure 5. Wind vectors and isotherms at 850 hPa for Mar. 9, 2006. The open triangle is Dunhuang and closed triangle denotes Minqin.

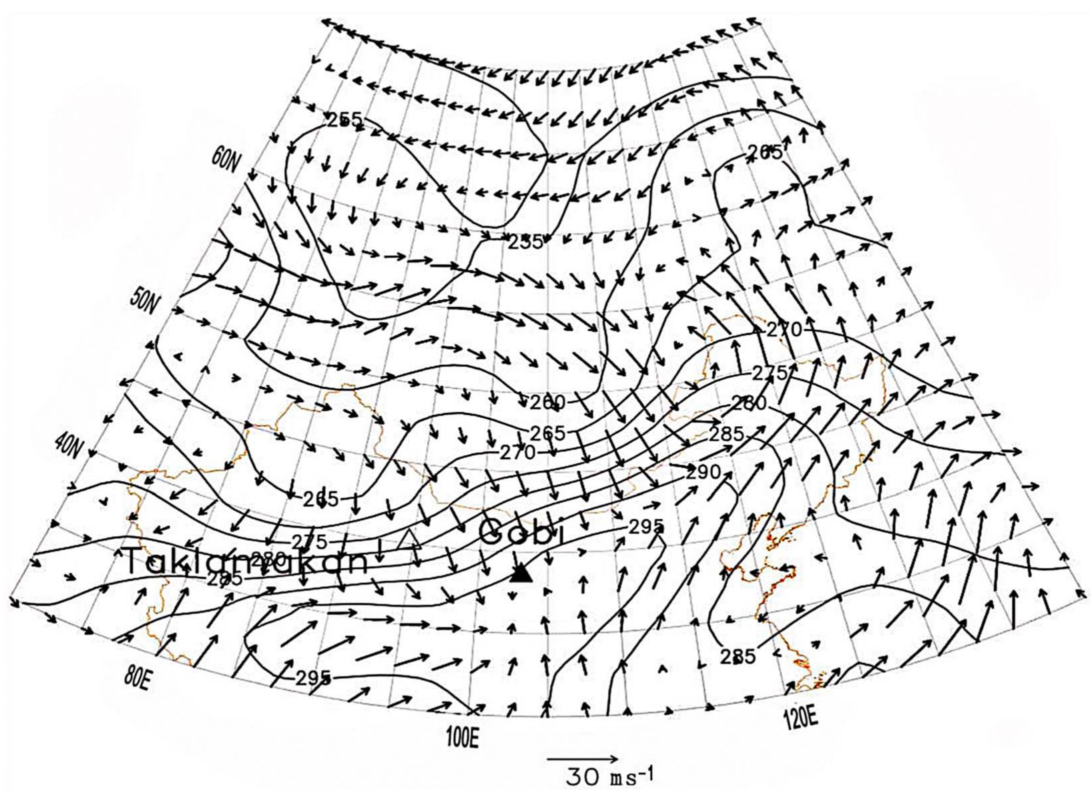

Figure 6. Similar to Figure 5 but for Apr. 10, 2006.

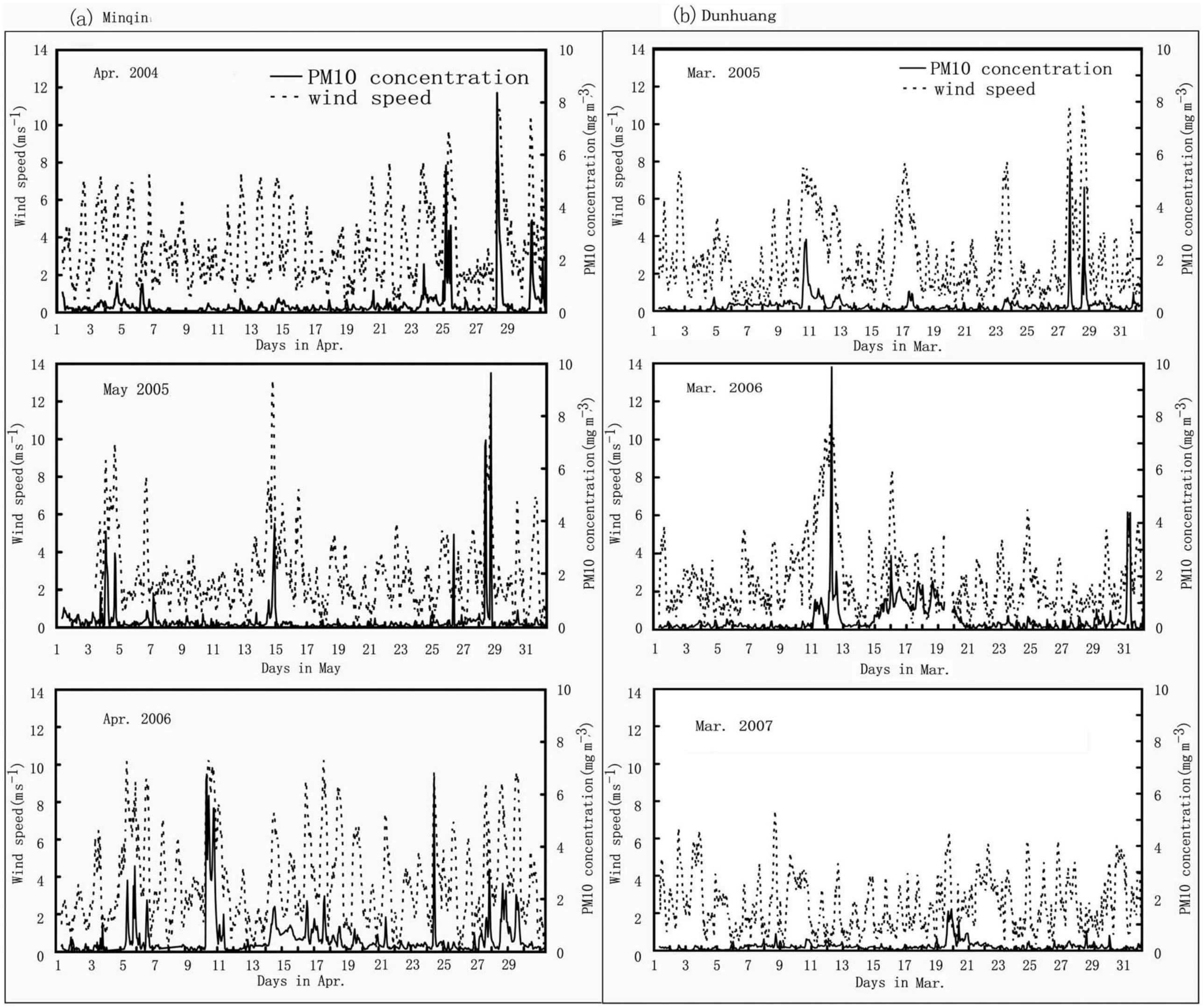

Figure 7. Time series of wind speed and PM_{10} concentration for (a) Minqin and (b) Dunhuang (hourly averaged).

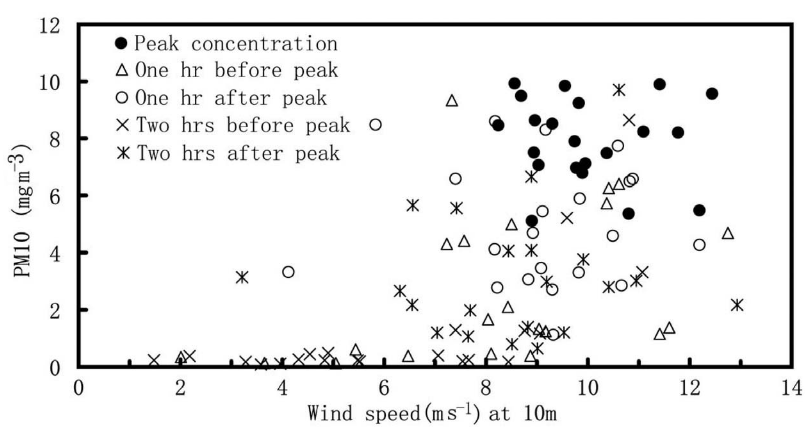

Figure 8. The peak PM_{10} concentration and the concentration values at 1 and 2 h before/after the peak value as a function of 10-m level wind speed for 21 dust storm events.

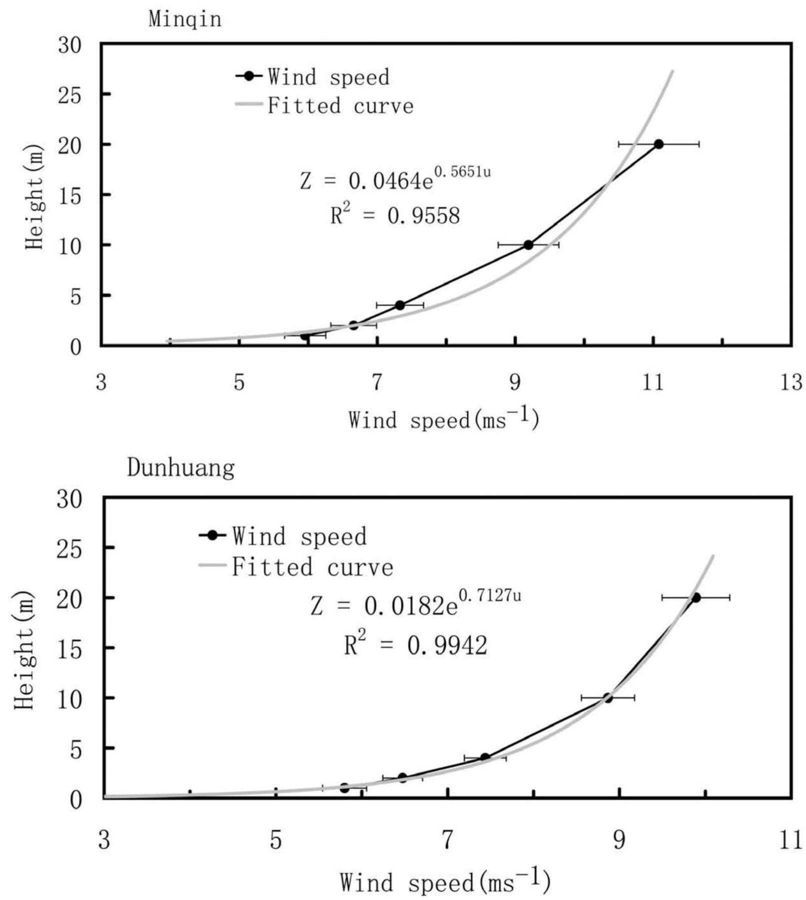

Figure 9. Wind profile under strong wind condition [u (10 m) > 8 m s^{-1}].

obtained the following formula for average velocity in the surface layer under neutral condition,

$$u = \frac{u_*}{k} \ln \frac{z}{z_0}. \quad (1)$$

where z_0 is aerodynamic roughness; $u_* = \sqrt{-\overline{u'w'}}$ is frictional velocity; $k = 0.4$ is *Von Karman* constant.

[28] Equation (1) can be rewritten as:

$$z = z_0 \cdot e^{\frac{k}{u_*} \cdot u} \quad (2)$$

Figure 9 shows wind speed as a function of height under strong wind condition (wind speed ≥ 8 m s^{-1} at 10-m level). The fitted curves correlate well with the averaged data. For Minqin and Dunhuang, the aerodynamic roughness z_0 = 0.046 m and z_0 = 0.018 m, and the friction velocity u_* = 0.71 m s^{-1} and u_* = 0.56 m s^{-1}, respectively during dust storms. Minqin has a rougher surface and stronger surface stress, which are due to uneven ground.

[29] Figure 10 presents the wind roses for the two sites under strong wind conditions. The winds were predominantly from northwest at Minqin, and were bidirectional from northeast or southwest at Dunhuang. The wind directions were distributed consistently with the north edge of the Tibetan Plateau (Figure 1).

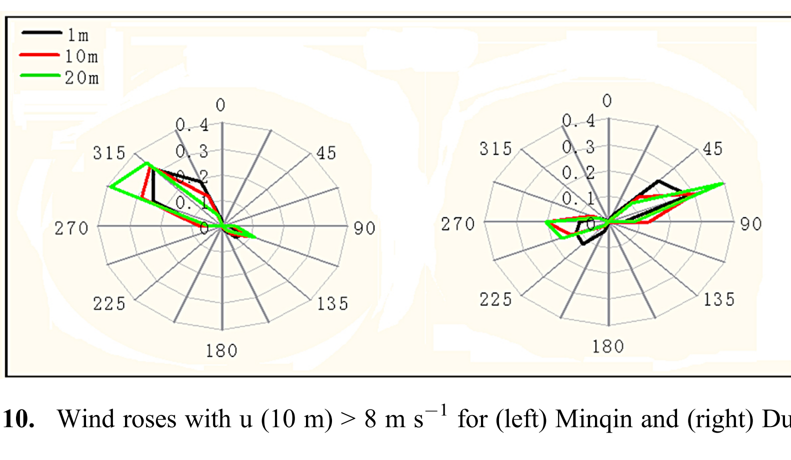

Figure 10. Wind roses with u (10 m) > 8 m s^{-1} for (left) Minqin and (right) Dunhuang.

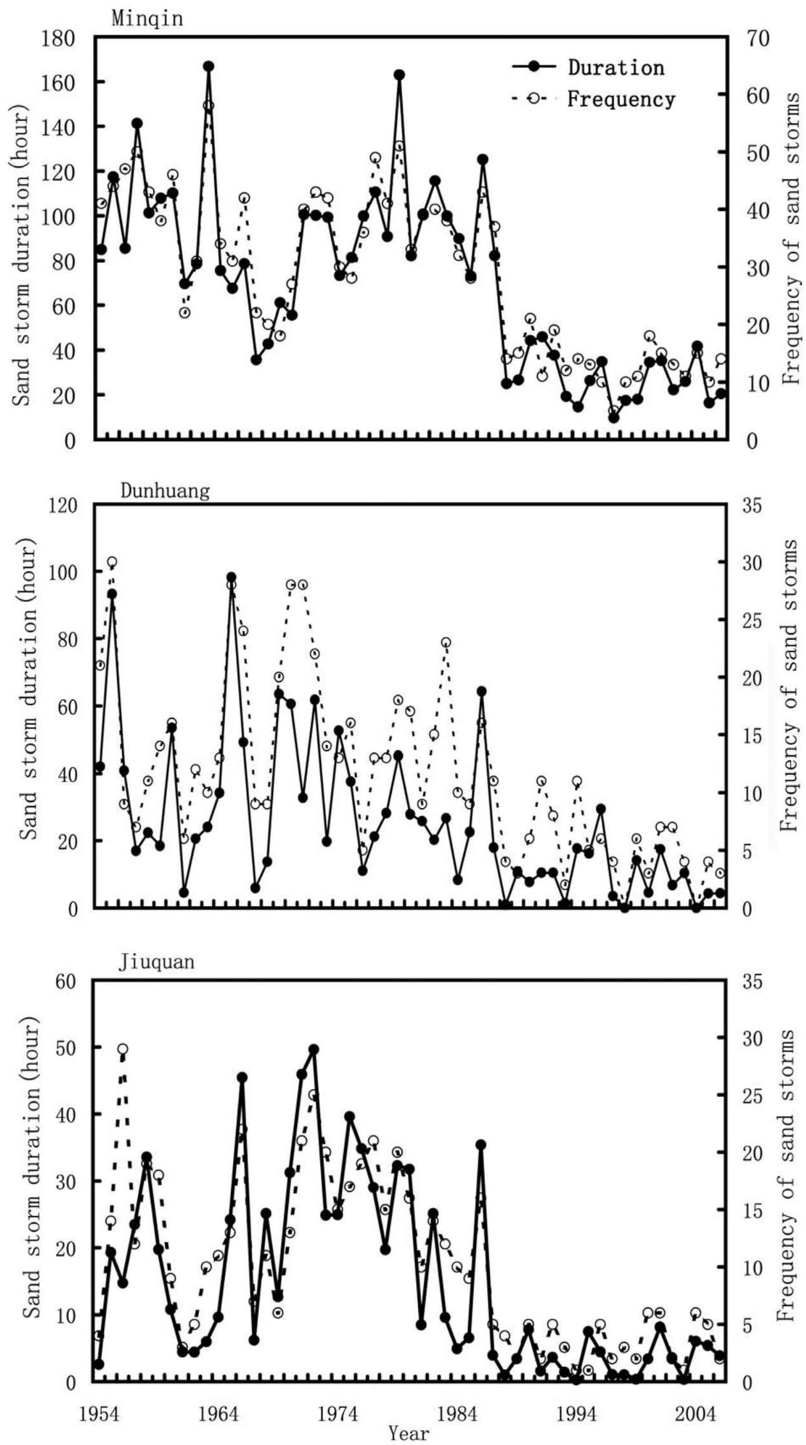

Figure 11. Annual durations of dust storms and annual frequency of dust storms for the period of 1954–2006 at (top) Minqin, (middle) Dunhuang and (bottom) Jiuquan.

3.4. Dust Storm Trend and the Wind Blowing Index

[30] Figure 11 shows annual dust storm duration and annual frequency of dust storms at Minqin, Duhuang and Jiuquan from 1954 to 2006 based on visual observations only. At all three sites, both the dust storm duration and frequency exhibit a declining trend. The interannual variability also appears to have declined over the 53 year period. Can the reduction of dust storms be explained by a change in meteorological conditions? Figure 12 shows time series of averaged wind speed and precipitation from 1954 through 2004 at Minqin. While the annual precipitation shows essentially no trend, the yearly average wind velocity appears to have a weak declining trend that is consistent with

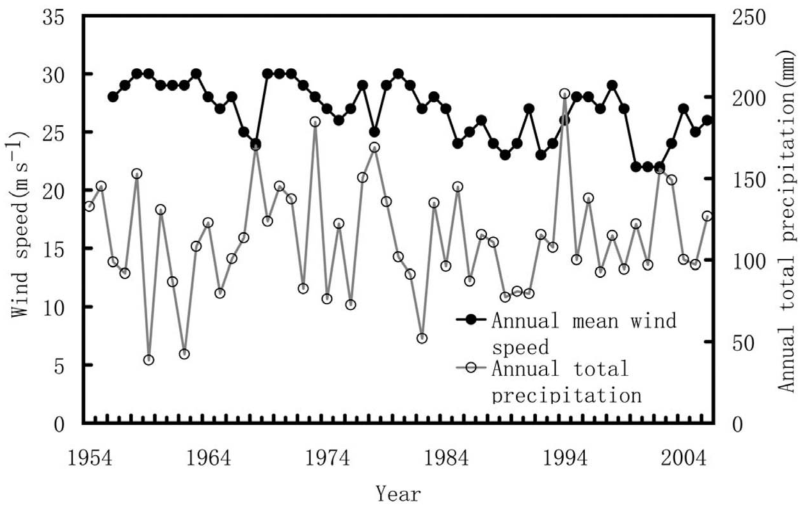

Figure 12. Annual mean surface wind speed and annual total precipitation at Minqin.

the trend in dust storm duration and frequency. The fact that the trend in wind speed is not nearly as strong as in dust storm properties may be explained by that the strong wind events causing dust storms are usually short-lived which contributed little to the yearly average of wind speed [*Engelstaedter and Washington*, 2007; *McGee et al.*, 2010]. *Qian and Zhang* [2007] have shown a reduction of the frequency and strengths of cold air outbreaks in the past decades, and they attributed this to the global warming and the variation of the atmospheric circulation internally. This led to a reduction of extremely windy days and thus the frequency and intensity of dust storms.

[31] In order to determine whether a declining trend of dust storms has some connection to climate change, we examine the wind blowing index (WBI). WBI is defined as the sum of possible events for dust storms, in which the northerly or northwesterly velocity is greater than 10 m s^{-1} at 850 hPa or 16 m s^{-1} at 700 hPa. Wind data from the NCEP global reanalysis data set [*Kalnay et al.*, 1996] are used to determine WBI in the past 50 years. Figure 13 shows WBI derived using 850 hPa and 700 hPa winds from 1954 to 2006. A decreasing trend in WBI seems to appear, which is consistent with the declining of the annual mean surface velocity and the trend of dust storms.

4. Conclusions

[32] Data from 50-year routine meteorological observations, NCEP reanalysis, and 3-year enhanced observations of aerosol and surface meteorology at three sites are analyzed to understand dust storm characteristics over the Gobi and Taklimakan Deserts, the source region of Asian dust storms, in northwest China.

[33] The results show that dust storms are more frequent over the Gobi Desert than the Taklimakan Desert. This is because the Gobi Desert is in the path of cold airflow from high latitudes to the south or southeast that often occur in the spring and winter, while the Taklimakan Desert is protected by mountain ranges from the invasion of this airflow.

[34] The aerosol characteristics, such as the mass concentration, scatter coefficient, and visibility are similar among the three observation sites during dust storms. The friction velocity and turbulence kinetic energy, however, are quite different, with much larger values during dust storm conditions than during quiescent conditions. The increase in

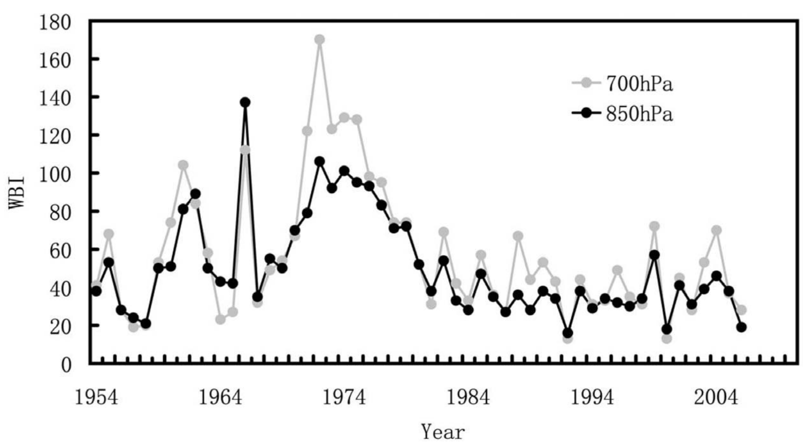

Figure 13. Variation of Wind Blowing Index WBI for 1954–2006 at Minqin.

turbulence is a result of mechanical generation due to stronger winds necessary to trigger dust storms. The lower atmosphere is near neutral during dust storms.

[35] There appears to be a decreasing trend in the frequency and duration of dust storms in the past 5 decades. This is consistent with the observed Arctic warming which decreases the frequency and intensity of cold air outbreaks that bring strong winds to the Gobi and the Taklimakan Deserts.

[36] **Acknowledgments.** The work was supported by National Science Foundation of China under grant 41175042 and the China Ministry of Education through the Fundamental Research Funds for the Central Universities LZUJBKY-2010-10, and the Development Program of Changjiang Scholarship and Research Team (IRT1018). This work was also jointly supported by the National Basic Research Program of China (2012CB955301) and National Science Foundation of China under grant 40725015. The authors would like to thank Cyrille Flamant and two anonymous reviewers for their insightful reviews of the original and revised manuscript.

References

Aoki, I., Y. Kurosaki, R. Osada, T. Sato, and F. Kimura (2005), Dust storms generated by mesoscale cold fronts in the Tarim Basin, northwest China, *Geophys. Res. Lett.*, *32*, L06807, doi:10.1029/2004GL021776.

Businger, J. A., J. C. Wyngaard, Y. Izumi, and E. F. Bradley (1971), Flux-profile relationships in the atmospheric surface layer, *J. Atmos. Sci.*, *28*, 181–189, doi:10.1175/1520-0469(1971)028<0181:FPRITA>2.0.CO;2.

Chen, B., H. Kitagawa, D. Jie, K. Hu, and J. Lim (2008), Dust transport from northeastern China inferred from carbon isotopes of atmospheric dust carbonate, *Atmos. Environ.*, *42*, 4790–4796, doi:10.1016/j.atmosenv.2008.01.057.

Dyer, A. J. (1974), A review of flux-profile relations, *Boundary Layer Meteorol.*, *7*, 363–372, doi:10.1007/BF00240838.

Engelstaedter, S., and R. Washington (2007), Temporal controls on global dust emissions: The role of surface gustiness, *Geophys. Res. Lett.*, *34*, L15805, doi:10.1029/2007GL029971.

Ge, J., J. Su, T. P. Ackerman, Q. Fu, J. Huang, and J. Shi (2010), Dust aerosol optical properties retrieval and radiative forcing over northwestern China during the 2008 China-U.S joint field experiment, *J. Geophys. Res.*, *115*, D00K12, doi:10.1029/2009JD013263.

Huang, J., P. Minnis, B. Lin, T. Wang, Y. Yi, Y. Hu, S. Sun-Mack, and K. Ayers (2006a), Possible influences of Asian dust aerosols on cloud properties and radiative forcing observed from MODIS and CERES, *Geophys. Res. Lett.*, *33*, L06824, doi:10.1029/2005GL024724.

Huang, J., B. Lin, P. Minnis, T. Wang, X. Wang, Y. Hu, Y. Yi, and J. R. Ayers (2006b), Satellite-based assessment of possible dust aerosols semi-direct effect on cloud water path over East Asia, *Geophys. Res. Lett.*, *33*, L19802, doi:10.1029/2006GL026561.

Huang, J., Y. Wang, T. Wang, and Y. Yi (2006c), Dusty cloud radiative forcing derived from satellite data for middle latitude region of East Asia, *Prog. Nat. Sci.*, *10*, 1084–1089.

Huang, J., P. Minnis, Y. Yi, Q. Tang, X. Wang, Y. Hu, Z. Liu, K. Ayers, C. Trepte, and D. Winker (2007), Summer dust aerosols detected from CALIPSO over the Tibetan Plateau, *Geophys. Res. Lett.*, *34*, L18805, doi:10.1029/2007GL029938.

Huang, J., P. Minnis, B. Chen, Z. Huang, Z. Liu, Q. Zhao, Y. Yi, and J. K. Ayers (2008), Long-range transport and vertical structure of Asian dust from CALIPSO and surface measurements during PACDEX, *J. Geophys. Res.*, *113*, D23212, doi:10.1029/2008JD010620.

Huang, J., Q. Fu, J. Su, Q. Tang, P. Minnis, Y. Hu, Y. Yi, and Q. Zhao (2009), Taklimakan dust aerosol radiative heating derived from CALIPSO observations using the Fu-Liou radiation model with CERES constraints, *Atmos. Chem. Phys.*, *9*, 4011–4021, doi:10.5194/acp-9-4011-2009.

Huang, J., P. Minnis, H. Yan, Y. Yi, B. Chen, L. Zhang, and J. K. Ayers (2010), Dust aerosol effect on semi-arid climate over northwest China detected from A-Train satellite measurements, *Atmos. Chem. Phys.*, *10*, 6863–6872, doi:10.5194/acp-10-6863-2010.

Huebert, B. J., T. Bates, P. B. Russell, G. Y. Shi, Y. J. Kim, K. Kawamura, G. Carmichael, and T. Nakajima (2003), An overview of ACE-Asia: Strategies for quantifying the relationships between Asian aerosols and their climatic impacts, *J. Geophys. Res.*, *108*(D23), 8633, doi:10.1029/2003JD003550.

In, H., and S. Park (2002), A simulation of long-range transport of yellow sand observed in April 1998 in Korea, *Atmos. Environ.*, *36*, 4173–4187, doi:10.1016/S1352-2310(02)00361-8.

Jigjidsuren, S., and S. Oyuntsetseg (1998), Pastureland utilization problems and ecosystem, in *Ecological Sustainable Development*, vol. 2, pp. 206–212, Admon, Ulaanbaatar.

Kalnay, E., et al. (1996), The NCEP/NCAR 40-Year Reanalysis Project, *Bull. Am. Meteorol. Soc.*, *77*, 437–471.

Kim, J. (2008), Transport routes and source regions of Asian dust observed in Korea during the past 40 years (1965–2004), *Atmos. Environ.*, *42*, 4778–4789, doi:10.1016/j.atmosenv.2008.01.040.

Kim, W., S. Doh, Y. Yu, and M. Lee (2008), Role of Chinese wind-blown dust in enhancing environmental pollution in Metropolitan Seoul, *Environ. Pollut.*, *153*, 333–341, doi:10.1016/j.envpol.2007.08.014.

Lee, C., A. Richter, H. Lee, Y. Kim, J. Burrows, Y. Lee, and B. Choi (2008), Impact of transport of sulfur dioxide from the Asian continent on the air quality over Korea during May 2005, *Atmos. Environ.*, *42*, 1461–1475, doi:10.1016/j.atmosenv.2007.11.006.

Li, X., and H. Zhang (2011), Research on threshold friction velocities during dust events over the Gobi Desert in northwest China, *J. Geophys. Res.*, *116*, D20210, doi:10.1029/2010JD015572.

Li, Z., L. Yue, X. Xue, M. Wang, L. Yang, H. Nie, and C. Chen (2006), Grain size distribution characteristics of different geogenetic types of sandy desertification and their geological significance in southeast MoUs desert (in Chinese), *Acta Sedimentol. Sin.*, *24*(2), 267–275.

McGee, D., W. Broecker, and G. Winckler (2010), Gustiness: The driver of glacial dustiness?, *Quat. Sci. Rev.*, *29*, 2340–2350, doi:10.1016/j.quascirev.2010.06.009.

Natsagdorj, L., D. Jugdera, and Y. S. Chung (2003), Analysis of dust storms observed in Mongolia during 1937–1999, *Atmos. Environ.*, *37*, 1401–1411, doi:10.1016/S1352-2310(02)01023-3.

Park, S., and H. In (2002), Simulation of long-range transport of acid pollutants in East Asia during the yellow sand event, *Atmos. Environ.*, *36*, 4877–4893, doi:10.1016/S1352-2310(02)00583-6.

Qian, W., and W. Zhang (2007), Changes in cold wave events and warm winter in China during the last 46 years, *Chin. J. Atmos. Sci.*, *31*, 1266–1278.

Qian, Z., Y. Cai, J. T. Liu, C. M. Liu, D. L. Li, and M. H. Song (2006), Some advances in dust storm research over China–Mongolia areas (in Chinese), *Chin. J. Geophys.*, *49*, 83–92.

Roberts, G., G. Mauger, O. Hadley, and V. Ramanathan (2006), North American and Asian aerosols over the eastern Pacific Ocean and their role in regulating cloud condensation nuclei, *J. Geophys. Res.*, *111*, D13205, doi:10.1029/2005JD006661.

Su, J., J. Huang, Q. Fu, P. Minnis, J. Ge, and J. Bi (2008), Estimation of Asian dust aerosol effect on cloud radiation forcing using Fu-Liou radiative model and CERES measurements, *Atmos. Chem. Phys.*, *8*, 2763–2771, doi:10.5194/acp-8-2763-2008.

Sun, J., M. Zhang, and T. Liu (2001), Spatial and temporal characteristics of dust storms in China and its surrounding regions, 1960–1999: Relations to source area and climate, *J. Geophys. Res.*, *106*(D10), 10,325–10,333, doi:10.1029/2000JD900665.

Tsai, Y. I., and C. Chen (2006), Characterization of Asian dust storm and non-Asian dust storm $PM_{2.5}$ aerosol in southern Taiwan, *Atmos. Environ.*, *40*, 4734–4750, doi:10.1016/j.atmosenv.2006.04.038.

VanCuren, R., and T. A. Cahill (2002), Asian aerosols in North America: Frequency and concentration of fine dust, *J. Geophys. Res.*, *107*(D24), 4804, doi:10.1029/2002JD002204.

Wang, W., J. Huang, P. Minnis, Y. Hu, J. Li, Z. Huang, J. K. Ayers, and T. Wang (2010), Dusty cloud properties and radiative forcing over dust source and downwind regions derived from A-Train data during the Pacific Dust Experiment, *J. Geophys. Res.*, *115*, D00H35, doi:10.1029/2010JD014109.

Wang, X., J. Huang, M. Ji, and K. Higuchi (2008), Variability of East Asia dust events and their long-term trend, *Atmos. Environ.*, *42*, 3156–3165, doi:10.1016/j.atmosenv.2007.07.046.

Westphal, D. L., O. B. Toon, and T. N. Carlson (1988), A case study of mobilization and transport of Saharan dust, *J. Atmos. Sci.*, *45*(15), 2145–2175, doi:10.1175/1520-0469(1988)045<2145:ACSOMA>2.0.CO;2.

Xuan, J., I. N. Sokolik, J. Hao, F. Guo, H. Mao, and G. Yang (2004), Identification and characterization of sources of atmospheric mineral dust in East Asia, *Atmos. Environ.*, *38*, 6239–6252, doi:10.1016/j.atmosenv.2004.06.042.

Yang, Q., L. Yang, G. Zhang, X. Li, H. Li, and W. Huo (2006), Research on classification of sandstorm intensity based on probability distribution of PM10 concentration, *J. Desert Res.*, *26*(2), 278–282.

Ye, D., J. Chou, J. Liu, Z. Zhang, Y. Wang, Z. Zhou, H. Ju, and H. Huang (2000), Causes of sand-stormy weather in northern China and control measures (in Chinese), *Acta Geogr. Sin.*, *55*(5), 513–521.

Zhang, X. (2001), Source distributions, emission, transportation, deposition of Asia dust and loess accumulation, *Quat. Sci.*, *21*, 29–40.